# Screening in $YBa_2Cu_3O_{7-\delta}$ at large wave vectors

Simo Huotari,[1] J. Aleksi Soininen,[2] György Vankó,[1,3] Giulio Monaco,[1] and Valerio Olevano[4]

[1] *European Synchrotron Radiation Facility, B.P. 220, F-38043 Grenoble cedex, France*
[2] *Department of Physics, P.O. Box 64, FI-00014 University of Helsinki, Finland*
[3] *KFKI Research Institute for Particle and Nuclear Physics, P. O. Box 49, H-1525 Budapest, Hungary*
[4] *Institut Néel, CNRS, B.P. 166, F-38042 Grenoble, France*

(Dated: November 8, 2010)

We present experimental inelastic x-ray scattering (IXS) and *ab initio* time-dependent density-functional-theory (TDDFT) studies of $YBa_2Cu_3O_{7-\delta}$. The response of the low-lying Ba $5p$ and Y $4p$ core electrons is shown to interact strongly with the Cu $3d$ and O $2p$ excitations, with important consequences on screening. The agreement between IXS and TDDFT results is excellent, apart from a new type of excitations, mainly related to loosely bound Ba electrons and significantly affected by correlations. This points to correlation mechanisms not fully described by TDDFT that might have a role in giving rise to antiscreening.

## I. INTRODUCTION

Despite 20 years of research since the discovery of cuprates as high-temperature superconductors (HTSC),[1] the nature of the superconductivity and the pairing mechanism in these systems still remain unknown. Extensive studies of HTSC cuprates have been done using the most varied techniques and on almost every observable imaginable. The dielectric function $\varepsilon(\mathbf{r},\mathbf{r}',t-t')$ is in particular a key quantity for superconductivity. Its inverse $\varepsilon^{-1}$ measures the screening of the bare Coulomb repulsion and can directly indicate reverse screening (antiscreening) spatial regions where the interaction between two electrons is attractive rather than repulsive. In these regions electrons pair up, giving rise to superconductivity. The study of $\varepsilon^{-1}$ can thus unambiguously indicate such domains and shed light to the pairing mechanism.

The dielectric function is probed often via its Fourier transform $\varepsilon(\mathbf{q},\omega)$ as in reflectance and ellipsometry spectroscopy, but usually only at negligible transferred momentum $|\mathbf{q}| = q \to 0$. This provides access only to long-range screening ($|\mathbf{r}-\mathbf{r}'| \to \infty$). In HTSC the coherence length is of the order of few inter-atomic distances [e.g. 1.5 nm in $YBa_2Cu_3O_{7-\delta}$ (YBCO) in the *ab* plane[2]]. The antiscreening domains have to exist at comparable or shorter distances. In the large-$q$ range, which would correspond to short-range correlations, experimental techniques are scarce due to the high-kinetic-energy particles required as a probe. As a consequence, this dynamic domain of $\varepsilon^{-1}(\mathbf{q},\omega)$ for $q > 0$ has been a no-man's land with very few applicable experimental probes. There are basically only two techniques available: the electron energy-loss (EELS) (Refs. 3 and 4) and inelastic x-ray scattering (IXS) (Ref. 5) spectroscopies. Both, in principle, measure the loss function, which is proportional to $-Im\left[\varepsilon^{-1}(\mathbf{q},\omega)\right]$. EELS, however, is inherently limited to relatively small values of $q$ due to an increasing multiple scattering at large wave vectors. IXS is left as the only technique probing exchanged wave vectors that correspond to inter-atomic distances, the typical range accessible to IXS being $q \gtrsim 5$ nm$^{-1}$. It can hence be a valuable technique to study HTSC.

IXS studies in strongly-correlated materials have been so far limited by the low count rates in high-$Z$ elements. Thanks to the rapid development in instrumentation, it is now becoming possible to apply IXS even to HTSC cuprates. Resonant IXS (Refs. 5–7) has already been used to study such systems but these experiments do not probe the dielectric function and should not be confused with non-resonant IXS which we use here. In particular on YBCO, EELS experiments[8–12] were performed soon after the discovery of its superconductivity, but there are no existing IXS experiments. This work is an attempt to close the gap in our accessible kinematic probing range of excitation energies and momenta.

The dominant theoretical picture on HTSC relies on the Hubbard model[13] and invokes a strong correlation mechanism to explain the pairing and the superconductivity in cuprates.[14] This model accounts only for the last unpaired electron of a copper atom and disregards all the complicated chemical, atomic and electronic structures of HTSC cuprates. They are supposed only to renormalize the two adjustable parameters of the model. Today, a good framework to search for a solution to the Hubbard model is the dynamical mean-field theory (DMFT) (Ref. 15) and more recently cellular DMFT which introduces a $\mathbf{k}$ dependence necessary to address the evident anisotropy in HTSC.[16,17] However, systematic improvements within this approach are difficult without introducing new adjustable parameters.

It has been recently demonstrated that *ab initio* theories can be applied to HTSC. Density-functional theory (DFT) has shown[18,19] its ability to reproduce the ground-state atomic structure of YBCO within its typical error $< 3\%$. However, DFT does not describe excited states. On the other hand, time-dependent density-functional theory (TDDFT) (Refs. 20 and 21) is in principle an *exact* theory to describe neutral excitations and the dielectric function. In practice, since the exact exchange-correlation functional of TDDFT is not available at the moment, approximations such as the adiabatic local-density approximation (TDLDA) (Ref. 22) are required. The latter has shown to provide loss-function spectra

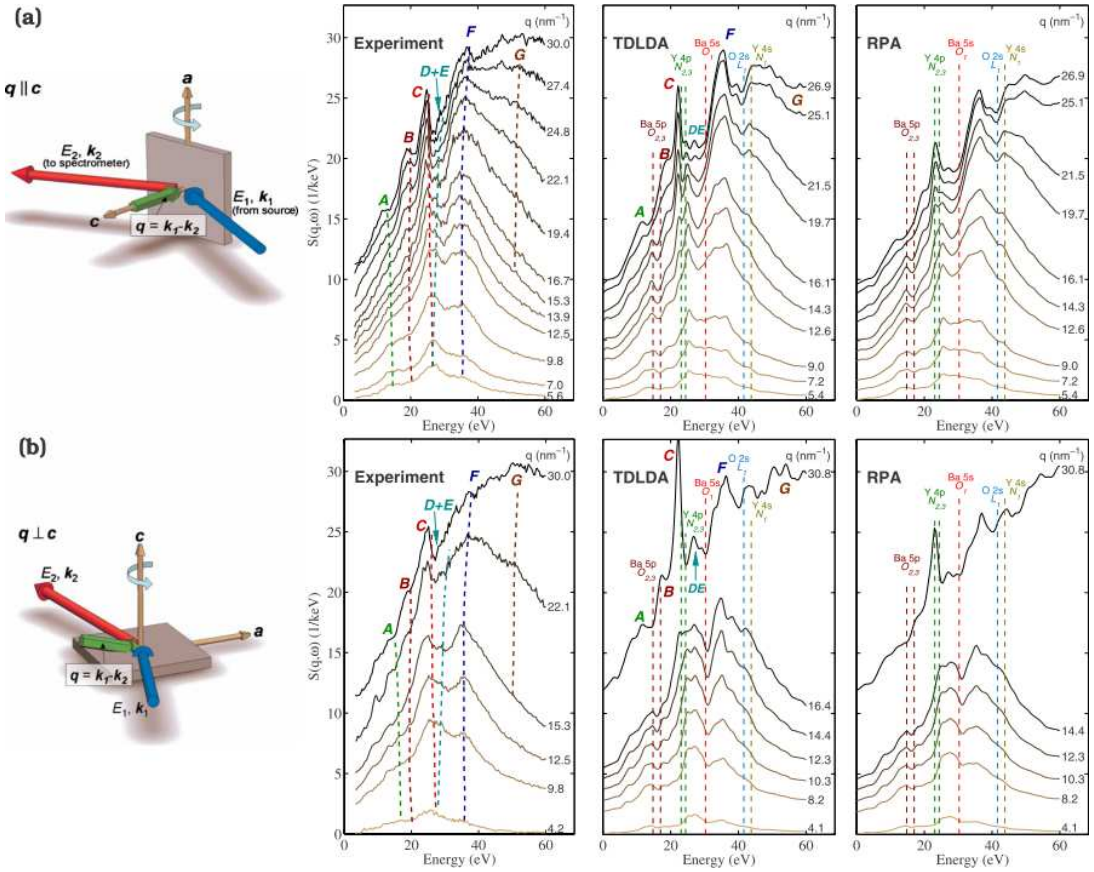


FIG. 1: Experimental and calculated energy-loss functions of YBCO for (a) $\mathbf{q} \parallel \mathbf{c}$ and (b) $\mathbf{q} \perp \mathbf{c}$. The most prominent spectral features are labeled $A$–$G$ and highlighted with dashed lines in the experimental plots. The nominal core-electron excitation energies are marked with dashed lines and labeled in the theory plots. For clarity, the spectra are shifted vertically from each other by an amount proportional to the corresponding momentum transfer value. Note that the experimental $S(\mathbf{q},\omega)$ are area-normalized to the TDLDA theory as described in the text. The experimental geometries for the two directions of $\mathbf{q}$ are shown on the left.

for ordinary semiconductors and insulators, e.g. silicon, in good agreement with both EELS (Ref. 23) and IXS (Ref. 24) experiments. Recent works have shown that TDLDA provides results in excellent agreement also with the exact solution of a one-dimensional Hubbard model, reproducing spin and charge collective excitations in a Luttinger liquid.[25,26] TDLDA can hence be a good formalism even in strongly correlated systems. However, so far there are no TDDFT studies of the dielectric function in cuprates.

In this work we present an investigation of the inverse dielectric function $\varepsilon^{-1}(\mathbf{q},\omega)$ on a prototypical high-temperature superconductor cuprate, $YBa_2Cu_3O_{7-\delta}$ ($\delta = 0.07$) combining IXS experiments with TDDFT calculations. IXS probes the dynamic structure factor $S(\mathbf{q},\omega)$, which is related to the dielectric function via

$$S(\mathbf{q},\omega) = -(\hbar q^2)/(4\pi^2 e^2 n)\ \mathrm{Im}\ \varepsilon^{-1}(\mathbf{q},\omega) \qquad (1)$$

$n$ being the electron density. We study $S(\mathbf{q} \parallel \mathbf{c},\omega)$ and $S(\mathbf{q} \perp \mathbf{c},\omega)$ for energies of 5–60 eV and $q$ between 5.6–30.0 nm$^{-1}$. The comparison of experimental results with TDDFT calculations provides an important benchmark for studying the electronic response of cuprates in the whole physically relevant momentum-transfer range. In particular, the large energy range studied here together with calculations facilitate the identification of the role of yttrium and barium in the valence electron dynamics of YBCO.

## II. EXPERIMENT

The non-resonant IXS measurements of the loss function of YBCO were done at the beamline ID16 (Refs. 27 and 28) of the European Synchrotron Radiation Facility (ESRF). The measurements were performed at room temperature using monochromatic x rays with energies of 7.9–8.0 keV. The spectrometer was based on a spherically bent Si(444) analyzer crystal in the Rowland-circle geometry. The bending radius of the crystal was 1 m and the Bragg angle was fixed to 89°. The spectrometer observed the intensity of scattered photons with a fixed

energy, and the energy transfer was tuned by changing the incident-photon energy. The sample was in a shape of a plaquette with a size of 5×5×0.1 mm$^3$, with the polished main face oriented perpendicular to the **c** axis and the edges along the **a** and **b** axes. The sample orientation was analyzed using a Laue photograph. The superconducting transition of the sample takes place at $T_C = 94$ K. The measurements were performed with $\mathbf{q} \parallel \mathbf{c}$ and with $\mathbf{q} \perp \mathbf{c}$. The measurement geometries in the two cases are shown in Fig. 1. While the sample is easy to align unambiguously for the measurements with $\mathbf{q} \parallel \mathbf{c}$, the measurements with $\mathbf{q} \perp \mathbf{c}$ were slightly more difficult with the sample in question. First of all, the usual twinning of a YBCO was present in the sample, giving a small amount of uncertainty to the exact directions of the **a** and **b** axes. While the measurements were performed as close to $\mathbf{q} \parallel \mathbf{a}$ as possible, for this reason we refer to these results rather as $\mathbf{q} \perp \mathbf{c}$. Furthermore, the measurement in the *ab* plane was done in a near-grazing incidence and near-grazing exit geometry. The incidence and exit angles were thus small but finite, giving a small **c** component to the momentum-transfer vector as shown in Fig. 1(b). However, this component was kept always smaller than the **q** resolution and thus is expected to have a negligible effect on the results.

All spectra at each fixed **q** were measured several times in the same conditions and after a normalization to the incident-beam intensity were found to be identical within statistical accuracy. The resulting spectra were then averaged in order to increase the statistical accuracy. This procedure minimizes the possibility for any experimental instabilities during the measurements. The resulting spectra, which at this stage are scattering intensities as a function of energy transfer $\omega$ and momentum transfer **q** were corrected for sample self-absorption and linear background. We refer to the $\mathbf{Q} = 0$ as the zone center, and thus momentum transfer values given below are absolute. The energy resolution of the experiment was 1.0 eV and the momentum-transfer resolution 1.5 nm$^{-1}$. The zero-energy-loss quasielastic line was subtracted by using an exponential fit to its positive-energy-transfer tail above 2.5 eV. This procedure yields reliable spectra above $\sim 3$ eV. The experimental spectra were normalized to the same area with the theoretical TDLDA spectra. Since in the current computational approach[29] the theoretical results are limited to values $q = \frac{2\pi}{nx}$, where $n$ is an integer and $x$ the length of the direct-space lattice vector, it was not necessarily possible to perform the calculation of $S(\mathbf{q}, \omega)$ exactly at all measured values of $q$. For the determination of the area-normalization factor, we first determined numerically the theoretical behavior of the integrated area $S_{\rm int}^{\rm theory}(q) = \int_0^{60{\rm eV}} S(q,\omega){\rm d}\omega$ and interpolated the resulting curve to the values of $q$ which were actually measured. A normalization to this area-integrated value yields finally the experimental $S(\mathbf{q}, \omega)$.

## III. THEORY

Our computational starting point was a standard ground-state DFT LDA calculation (as in Ref. 18) of the total energy and the electronic density in YBCO using the ABINIT code.[30] A plane-wave basis set was used with a converged 160 Ry kinetic-energy cutoff and periodic boundary conditions. As turns out later to be very important, we included the low-lying-core states Ba 5*s*5*p*, Y 4*s*4*p*, Cu 3*s*3*p*, and O 2*s* in the valence using Hartwigsen-Goedecker-Hutter pseudopotentials. Employing the calculated DFT Kohn-Sham energies and wave functions we carried out a TDDFT calculation of the polarizability and the dielectric function using the DP code,[29] using both TDLDA and random phase approximation (RPA). The latter neglects correlation effects in the dielectric response of the system, and the comparison of TDLDA and RPA might give a hint where correlation effects play an important role. The independent-particle polarizability was constructed summing over 350 Kohn-Sham bands calculated at a Monkhorst-Pack $8 \times 8 \times 3$ $k$-point grid shifted by ($\frac{1}{2}$ $\frac{1}{2}$ $\frac{1}{2}$). The dimensions of polarizabilities and longitudinal dielectric functions as matrices in the reciprocal space were 347×347. The inversion of the polarizability matrix produces so-called local field effects where different excitation channels mix. This effect, usually neglected in the localized description, is well known from earlier first-principles studies on, e.g., transition metals.[31] It should be emphasized that we found these local-field effects to be crucial to obtain a good agreement between experiment and theory and should definitely not be neglected in this system. We used experimental lattice parameters, and we verified that the relaxed theoretical atomic structure[18] produces only minor changes to the spectra. All theoretical data shown here were convoluted with the experimental resolution function.

## IV. RESULTS AND DISCUSSION

The measured and calculated spectra are shown in Fig. 1. The agreement between the experimental and theoretical results is remarkably good. This is a manifestation that the TDDFT is an extremely useful tool in understanding the physics of even this canonical strongly correlated system. In fact, all relevant physics of the electronic excitations studied here are captured by the TDDFT. The energy range of the investigated excitations covers the collective oscillations of the valence electrons (plasmons), consisting mostly of the hybridized Cu 3*d* and O 2*p*, and the excitations of shallow core electrons of Y and Ba. Because the latter interact strongly with the valence electrons due to the important overlap in energy, we call them *semicore states*. The literature values[32,33] for their atomic excitation energies are 14.8 eV (Ba $5p_{3/2}$), 17.0 eV (Ba $5p_{1/2}$), 23.1 eV (Y $4p_{3/2}$), 24.4 eV (Y $4p_{1/2}$), 30.3 eV (Ba 5*s*), 41.6 eV (O 2*s*) and 43.8 eV (Y 4*s*). These are

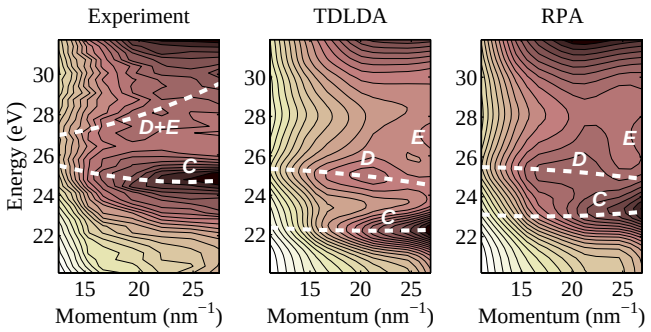


FIG. 2: Zoom-up to the region of 20–32 eV energy transfer to show the Ba $5p$ + Y $4p$ related dispersing excitations $C$–$E$ in experiment, TDLDA and RPA. Their dispersion are marked with dashed lines as a guide for eyes.

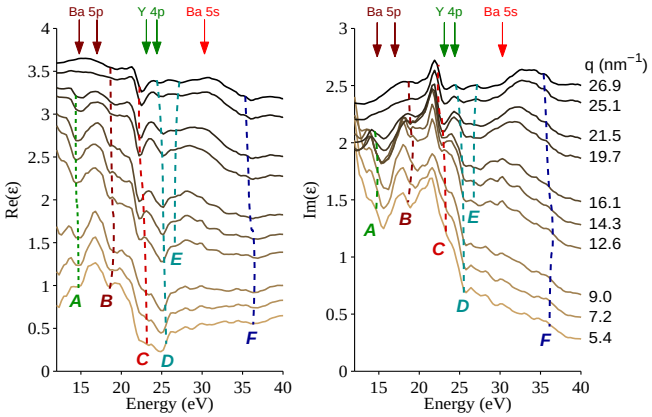


FIG. 3: The real part (left) and imaginary part (right) of the dielectric function as calculated within the TDLDA for the $\mathbf{q} \parallel \mathbf{c}$ direction. The excitation dispersions are labeled as in Fig. 1 and nominal core-excitation thresholds are annotated on top.

marked in the Fig. 1 with dashed lines. Assuming that these electrons indeed are strongly bound, they can only be excited above these energies. Measuring the spectra at these core-electron excitation thresholds to unoccupied states above the Fermi level bears resemblance to soft x-ray absorption spectra of those core electrons. This scattering process is called x-ray Raman scattering, and has been used successfully to measure soft x-ray absorption spectra of low-lying core electrons edge even in high pressure environments, accessible by the high-energy x-rays used in the experiment.[34,35]

The IXS spectra in this regime are similar to those that could be studied by EELS except for the important possibility to access large momentum transfers (up to 25 nm$^{-1}$ in this study but in principle unlimited). For example, an early EELS study of YBCO has revealed spectra equivalent to those reported here at the lowest $q$ (Ref. 12). The anisotropy between the $ab$ plane and the $c$-axis results is surprisingly small in the experiment. Meanwhile, the theory (both within TDLDA and RPA) would predict a slightly larger anisotropy,[36] at least between the calculated **a** and **c** directions.

The spectral features found here are labeled with letters $A$–$G$ in Fig. 1. The features $A$ and $B$ correspond to the excitation of the Ba $5p$ electrons (the Ba $O_{2,3}$ absorption edges). The features $C$–$E$ are rather intriguing. The relevant $S(q,\omega)$ range for the case of $\mathbf{q} \parallel \mathbf{c}$ is showed zoomed-up in the Fig. 2, in both TDLDA and RPA together with the experiment. It is in this region where the differences of TDLDA and RPA are the most pronounced. In RPA the peaks $D$ and $E$ are broad and weak, but appear better defined in TDLDA. On the other hand, experimentally there are only two excitations, which we label tentatively as $C$ and $D+E$ since it seems that the peaks $D+E$ have merged together within the experimental accuracy. All these peaks appear at higher energies in the experiment than in the theory. The energies of the excitations $C$–$E$ disperse with momentum transfer, for the excitations $D+E$ most strongly in the experimental result. As a guide for the eyes, their dispersion is marked with dashed lines in Fig. 1. In the experiment $C$ and $D+E$ seem to coalesce into a single peak at low momentum transfer. To observe these excitations separately, an access to large momentum transfers is essential, in particular since it seems that the peak $E$ starts gaining considerable spectral weight only for $q > 20$ nm$^{-1}$. These peaks are reproduced by the theory in both approximations but a clear discrepancy between experiment and theory remains. In particular in the experiment the excitation $D+E$ seems to follow a quadratic dispersion typical for a plasmon, a trend not reproduced by theory even if TDLDA reproduces the excitations better. *This could be one of the key differences where a treatment of correlations beyond TDLDA is necessary.*[37,38] These excitations are sensitive to correlation, as suggested by the evident differences between the two exchange-correlation approximations. It would seem natural to assign them to Y $4p$ which has an excitation threshold in the same energy. However, surprisingly, by occupation analysis we have found them to originate mostly from Ba $5p$ instead. As the wave functions of these excited states overlap with those of Y $4p$, the interaction of Ba $5p$ and Y $4p$ excitations seems to be strong. Finally the features $F$ and $G$ are related to the Ba $5s$ and Y $4s$ + O $2s$ excitations, respectively.

The dielectric function as calculated within the TDLDA is shown in Fig. 3 for the $\mathbf{q} \parallel \mathbf{c}$ direction. Any single-particle excitation, associated to a transition of a single electron from an occupied to an empty state, should be apparent as a peak in Im($\varepsilon$). The position of such an excitation corresponds to the transition energy between the two states of the band-like picture, eventually renormalized by electron-electron interaction effects (single-quasiparticle[39] excitations) and electron-hole (excitonic[40,41]) effects.

On the other hand, collective plasmon excitations would manifest themselves as zero-crossings of the real part of the dielectric function Re($\varepsilon$), when the imagi-

nary part Im($\varepsilon$) is small. These frequencies are in correspondence with the self-sustained resonant modes of the system, associated to collective oscillations of the electron plasma. When the plasmon is strongly damped (usually due to an interaction with single-particle excitations), the zero-crossing disappears but a relict may remain as a minimum of Re($\varepsilon$). Here we find no zero-crossings of Re($\varepsilon$) in agreement with earlier studies,[12] implying that the plasmons in this system are heavily damped. While the peaks *A*–*C* are produced by dips in the real part at low $q$, they change their character into a peak in the imaginary part at highest $q$ studied here, showing a transition from a highly-damped plasmon to a single-particle excitation as $q$ is increased. The peak *D* has the clearest damped-plasmon-type character with the largest minimum in Re($\varepsilon$) at low $q$. While much of the spectral weight is due to the Cu 3*d* and O 2*p*, most of the fine structure is in fact due to the Y 4*p* and Ba 5*p* electrons. By occupation analysis we have identified the peaks *A*–*D* to originate from Ba 5*p*, but especially at the largest momentum transfers the Y 4*p* single-particle core excitations overlap with the excitation *D*. In other words the Y 4*p* and Ba 5*p* core excitations interact strongly with the Cu 3*d* + O 2*p* valence excitations. For the peak *E* there is a weak peak in Im($\varepsilon$) at the corresponding energy and momentum, suggesting a single-electron type excitation for this peak, mostly Y 4*p* character.

A surprising aspect in the charge response of YBCO in this energy range is that it seems to fall outside the above-described normal separation between collective and single-particle excitations, and rather has a peculiar mixed character. For instance, we found that at low $q$ the changes in Re($\varepsilon$) due to Ba 5*p*, often considered as a core state, seem to be indispensable for obtaining a quantitative agreement between the theory and the experiment. The Ba 5*p* excitations introduce new minima in Re($\varepsilon$) around 25 eV reducing its value by approximately 50%, giving a large contribution to the collective *C*-*D* excitations at low $q$. Furthermore, below 20 eV the Ba 5*p* electrons increase the value of Re($\varepsilon$) and decrease the spectral weight in this energy range in the final loss function. This is even true below 10 eV where the increase in Re($\varepsilon$) is approximately 10%. However, at $q \gtrsim 20\text{nm}^{-1}$ their response is seen as peaks in Im($\varepsilon$), indicating in turn typical core-electron excitations. On the contrary, the Y 4*p* excitations have mostly a single-particle character at all values of $q$ studied here. Nevertheless, they have a significant role in determining the final shape of the loss function.

The results shown here are a clear proof that the valence dynamics of YBCO cannot be described in detail by considering only the Cu 3*d* and O 2*p*, but at least the Ba 5*p* and Y 4*p* have to be taken into account. Besides hybridizing, they couple to the Cu 3*d* + O 2*p* through the local field effect and they may be important also at much lower energies than the ones investigated here.

All real electronic systems, and even the jellium model, exhibit damping of the collective excitations at increased wave vectors — a result well known from Landau's theory (see for instance the discussion in Refs. 42 and 43 and references therein). One of the reasons for the plasmon damping is the coupling to single-particle electron-hole pair excitations. In simple metals the effect of single-particle excitations on the plasmon linewidth has been studied using, e.g., nearly-free-electron approach[44] as well as more recently using an *ab initio* method.[45] In all cases where single-particle excitation channels are strong in the range of plasmon energies, the damping will be more severe than in the jellium model. This is exactly the reason why a single-band theory cannot describe this situation: all electronic excitation pathways, which depend very much on the full band structure, have to be taken into account equally. In the cuprates and other so-called strongly correlated systems this may not be a trivial task. Even excitations of semicore electrons can play an important role in the damping of collective excitations, as we have shown in YBCO. On the other hand, it is not yet clear whether the band-like paradigm still holds for the highest occupied valence levels in these systems. This was exactly the motivation for the current work. We have shown here that *ab initio* TDDFT can describe a complicated system like YBCO and increase our understanding of the interplay between semicore and valence electrons.

## V. CONCLUSIONS

In conclusion, we have presented a combined experimental and theoretical study of the dielectric function of YBCO for large wave vectors, probing small interparticle distances. This previously unexplored area of studies reveals new interactions between Cu 3*d* and O 2*p* valence excitations with the weakly bound Ba 5*p* and Y 4*p* electrons in the dynamic response and screening. Especially the role of Ba 5*p* is found to be of mixed single-particle and damped-collective type giving rise to a novel excitation, observable only at large wave vectors, suggesting its importance in screening at short distances. We have shown that the valence dynamics interacts strongly with the low-lying semicore states. We have answered as well the question of how well we are able to model a HTSC cuprate system with many-particle interactions of the valence electrons that invalidate the band structure picture. In fact, against all expectations, *ab initio* TDDFT proves to be a valid and powerful theory to describe a HTSC cuprate and gives results which agree with the experiment very well. Finally, it is possibly in the remaining differences between the experiment and theory presented in this work where the effects of strong correlations, and perhaps even the origin of the Cooper pairing, could be looked for.

Beamtime was granted by ESRF and computing time by Ciment via NanoSTAR. J.A.S. acknowledges the Magnus Ehrnrooth foundations support for this research and Academy of Finland (Contracts No. 1110571 and

1127462). G.V. acknowledges financial support from the Hungarian Research Fund (OTKA, contract No. K 72597) and from the Bolyai Janes program of the Hungarian Academy of Sciences. The authors would like to thank Roberto Verbeni and Christian Henriquet for their support.

[1] J. G. Bednorz and K. A. Müller, Z. Phys. B **64**, 189 (1986).
[2] W. Buckel and R. Kleiner, *Superconductivity* (Wiley, Weinheim, 2004).
[3] J. Fink, Adv. Electron. Electron Phys. **75**, 121 (1989).
[4] F. J. García de Abajo, Rev. Mod. Phys. **82**, 209 (2010).
[5] W. Schülke, *Electron Dynamics by Inelastic X-Ray Scattering* (Oxford University Press, Oxford, 2007).
[6] K. Ishii, K. Tsutsui, Y. Endoh, T. Tohyama, K. Kuzushita, T. Inami, K. Ohwada, S. Maekawa, T. Masui, S. Tajima, et al., Phys. Rev. Lett. **94**, 187002 (2005).
[7] A. Kotani and S. Shin, Rev. Mod. Phys **73**, 203 (2001).
[8] A. Balzarotti, M. De Crescenzi, N. Motta, F. Patella, and A. Sgarlata, Solid State Comm. **68**, 381 (1988).
[9] C. H. Chen, L. F. Schneemeyer, S. H. Liou, M. Hong, J. Kwo, H. S. Chen, and J. V. Waszczak, Phys. Rev. B **37**, 9780 (1988).
[10] J. Yuan, L. M. Brown, and W. Y. Liang, J. Phys. C: Solid State Phys. **21**, 517 (1988).
[11] C. Tarrio and S. E. Schnatterly, Phys. Rev. B **38**, 921 (1988).
[12] H. Romberg, N. Nücker, J. Fink, T. Wolf, X.-X. Xi, B. Koch, H. P. Geserich, M. Durrler, W. Assmus, and B. Gegenheimer, Z. Physik B: Cond. Matter **78**, 367 (1990).
[13] P. W. Anderson, Science **235**, 1196 (1987).
[14] A.-M. S. Tremblay, B. Kyung, and D. Sénéchal, Low Temp. Phys. **32**, 424 (2006).
[15] A. Georges, G. Kotliar, W. Krauth, and M. J. Rozenberg, Rev. Mod. Phys. **68**, 13 (1996).
[16] M. Civelli, M. Capone, S. S. Kancharla, O. Parcollet, and G. Kotliar, Phys. Rev. Lett. **95**, 106402 (2005).
[17] M. Civelli, Phys. Rev. B **79**, 195113 (2009).
[18] R. Kouba, C. Ambrosch-Draxl, and B. Zangger, Phys. Rev. B **60**, 9321 (1999).
[19] H. Khosroabadi, B. Mossalla, and M. Akhavan, Phys. Rev. B **70**, 134509 (2004).
[20] E. Runge and E. K. U. Gross, Phys. Rev. Lett **52**, 997 (1984).
[21] E. K. U. Gross and W. Kohn, Phys. Rev. Lett. **55**, 2850 (1985).
[22] A. Zangwill and P. Soven, Phys. Rev. A **21**, 1561 (1980).
[23] V. Olevano, M. Palummo, G. Onida, and R. Del Sole, Phys. Rev. B **60**, 014224 (1999).
[24] H. C. Weissker, J. Serrano, S. Huotari, F. Bruneval, F. Sottile, G. Monaco, M. Krisch, V. Olevano, and L. Reining, Phys. Rev. Lett. **97**, 237602 (2006).
[25] C. Verdozzi, Phys. Rev. Lett. **101**, 166401 (2008).
[26] W. Li, G. Xianlong, C. Kollath, and M. Polini, Phys. Rev. B **78**, 195109 (2008).
[27] R. Verbeni, T. Pylkkänen, S. Huotari, L. Simonelli, G. Vankó, K. Martel, C. Henriquet, and G. Monaco, J. Synchrotron Radiat. **16**, 469 (2009).
[28] S. Huotari, G. Vankó, F. Albergamo, C. Ponchut, H. Graafsma, C. Henriquet, R. Verbeni, and G. Monaco, J. Synchrotron Radiat. **12**, 467 (2005).
[29] http://www.dp-code.org.
[30] http://www.abinit.org.
[31] I. G. Gurtubay, J. M. Pitarke, W. Ku, A. G. Eguiluz, B. C. Larson, J. Tischler, P. Zschack, and K. D. Finkelstein, Phys. Rev. B **72**, 125117 (2005).
[32] J. C. Fuggle and N. Mårtenson, J. El. Spectrosc. Relat. Phenom. **21**, 275 (1980).
[33] M. Cardona and L. Ley, eds., *Photoemission in Solids I: General Principles* (Springer-Verlag, Berlin, 1978).
[34] T. Pylkkänen, V. M. Giordano, J. C. Chervin, A. Sakko, M. Hakala, J. A. Soininen, K. Hämäläinen, G. Monaco, and S. Huotari, J. Phys. Chem B. **114**, 3804 (2010).
[35] S. K. Lee, J.-F. Lin, Y. Q. Cai, N. Hiraoka, P. J. Eng, T. Okuchi, H.-K. Mao, Y. Meng, M. Y. Hu, P. Chow, et al., Proc. Nat. Acad. Sci. **105**, 7925 (2008).
[36] S. Botti, N. Vast, L. Reining, V. Olevano, and L. C. Andreani, Phys. Rev. Lett. **89**, 216803 (2002).
[37] F. Sottile, F. Bruneval, A. G. Marinopoulos, L. K. Dash, S. Botti, V. Olevano, N. Vast, A. Rubio, and L. Reining, Int. J. Quantum Chem. **102**, 684 (2005).
[38] R. Del Sole, G. Adragna, V. Olevano, and L. Reining, Phys. Rev. B **67**, 045207 (2003).
[39] G.-M. Rignanese, X. Blase, and S. G. Louie, Phys. Rev. Lett. **86**, 2110 (2001).
[40] S. Albrecht, L. Reining, R. Del Sole, and G. Onida, Phys. Rev. Lett. **80**, 4510 (1998).
[41] S. Albrecht, L. Reining, G. Onida, V. Olevano, and R. Del Sole, Phys. Rev. Lett. **83**, 3971 (1999).
[42] S. Galambosi, J. A. Soininen, A. Mattila, S. Huotari, S. Manninen, G. Vankó, N. D. Zhigadlo, J. Karpinski, and K. Hämäläinen, Phys. Rev. B **71**, 060504(R) (2005).
[43] S. Huotari, C. Sternemann, M. C. Troparevsky, A. G. Eguiluz, M. Volmer, H. Sternemann, H. Müller, G. Monaco, and W. Schülke, Phys. Rev. B **80**, 155107 (2009).
[44] K. Sturm and L. E. Oliveira, Phys. Rev. B **24**, 3054 (1981).
[45] A. G. Eguiluz, W. Ku, and J. M. Sullivan, J. Phys. Chem. Solids **61**, 383 (2000).